ACS OMEGA

Open Access

http://pubs.acs.org/journal/acsodf

Article

AlbuCatcher for Long-Acting Therapeutics

Ji Hyun Rho, Jae Hun Lee, and Inchan Kwon*

Cite This: *ACS Omega* 2024, 9, 22990−23000

Read Online

ACCESS | Metrics & More | Article Recommendations | Supporting Information

ABSTRACT: Therapeutic proteins, pivotal for treating diverse human diseases due to their biocompatibility and high selectivity, often face challenges such as rapid serum clearance, enzymatic degradation, and immune responses. To address these issues and enable prolonged therapeutic efficacy, techniques to extend the serum half-life of therapeutic proteins are crucial. The AlbuCatcher, a conjugate of human serum albumin (HSA) and SpyCatcher, was proposed as a general technique to extend the serum half-life of diverse therapeutic proteins. HSA, the most abundant blood protein, exhibits a long intrinsic half-life through Fc receptor (FcRn)-mediated recycling. The SpyTag/SpyCatcher (ST/SC) system, known for forming irreversible isopeptide bonds, was employed to conjugate HSA and therapeutic proteins. Site-specific HSA conjugation to SC was achieved using an inverse electron-demand Diels−Alder (IEDDA) reaction, minimizing activity loss. Using urate oxidase (Uox) as a model protein with a short half-life, the small ST was fused to generate Uox-ST. Then, HSA-conjugated Uox (Uox-HSA) was successfully prepared via the Uox-ST/AlbuCatcher reaction. In vitro enzyme assays demonstrated that the impact of ST fusion and HSA conjugation on Uox enzymatic activity is negligible. Pharmacokinetics studies in mice revealed that Uox-HSA exhibits a significantly longer serum half-life (about 18 h) compared to Uox-WT (about 2 h). This extended half-life is attributed to FcRn-mediated recycling of HSA-conjugated Uox, demonstrating the effectiveness of the AlbuCatcher strategy in enhancing the pharmacokinetics of therapeutic proteins.

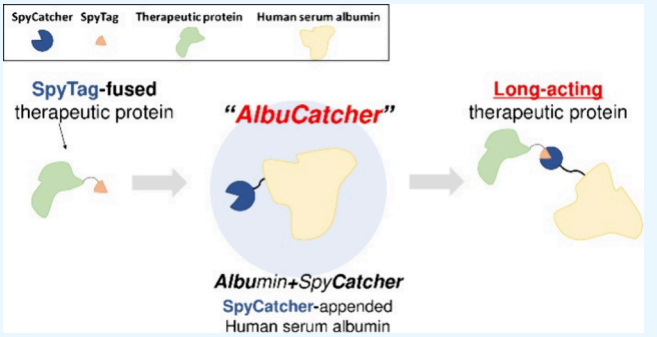

INTRODUCTION

Therapeutic proteins play a pivotal role in treating a wide range of human diseases due to their biocompatibility and high selectivity compared to small-molecule-based drugs.[1] Nonetheless, therapeutic proteins face challenges of rapid serum clearance through renal filtration, enzymatic degradation, and immune response.[2] Consequently, frequent administration to sustain therapeutic efficacy over prolonged periods of time demanded techniques to extend the serum half-life of therapeutic proteins.

Human serum albumin (HSA) is the most abundant protein in human blood, with a molecular weight of approximately 67 kDa. HSA exhibits a remarkably long intrinsic half-life by evading intracellular degradation through the neonatal Fc receptor (FcRn)-mediated recycling (Figure 1A).[3,4] Furthermore, its low immunogenicity and biodegradability have led to research exploring its potential as a half-life extender. Genetic fusion[5−7] or chemical conjugation[8−10] of HSA to therapeutic proteins successfully extended the serum half-life. However, the genetic fusion of HSA requires the development of the purification process for each fused therapeutic protein, which is very time-consuming. Furthermore, the HSA fusion may not be the best option for some therapeutic proteins, such as urate oxidase (Uox) and asparaginase, expressed in *Escherichia coli*, because HSA is not efficiently expressed in *E. coli* due to multiple disulfide bonds. Direct conjugation of macromolecules, such as HSA and poly(ethylene glycol), to therapeutic proteins often results in significant activity loss, because these macromolecules can block the critical sites of therapeutic proteins.[5,6,11,12] Therefore, developing alternative technologies to enhance the pharmacokinetics of diverse therapeutic proteins is still important.

The SpyTag/SpyCatcher (ST/SC) system is a protein coupling tool known for its ability to spontaneously form an irreversible isopeptide bond. The reaction occurs between the aspartic acid residue of the peptide ST and the lysine residue within the protein SC, which is facilitated by the catalytic glutamic acid also present in SC. Through engineering involving screening of phage libraries and rational design, the third-generation ST/SC attained a high reaction rate and reactivity.[13−15] Since both ST and SC can be expressed in *E. coli*, their fusion to therapeutic proteins can also be expressed in diverse hosts including *E. coli*. In this study, we explored a novel technology, AlbuCatcher, for generating long-acting therapeutic proteins. AlbuCatcher is the conjugate of HSA and

Received: March 9, 2024
Revised: April 24, 2024
Accepted: May 7, 2024
Published: May 13, 2024

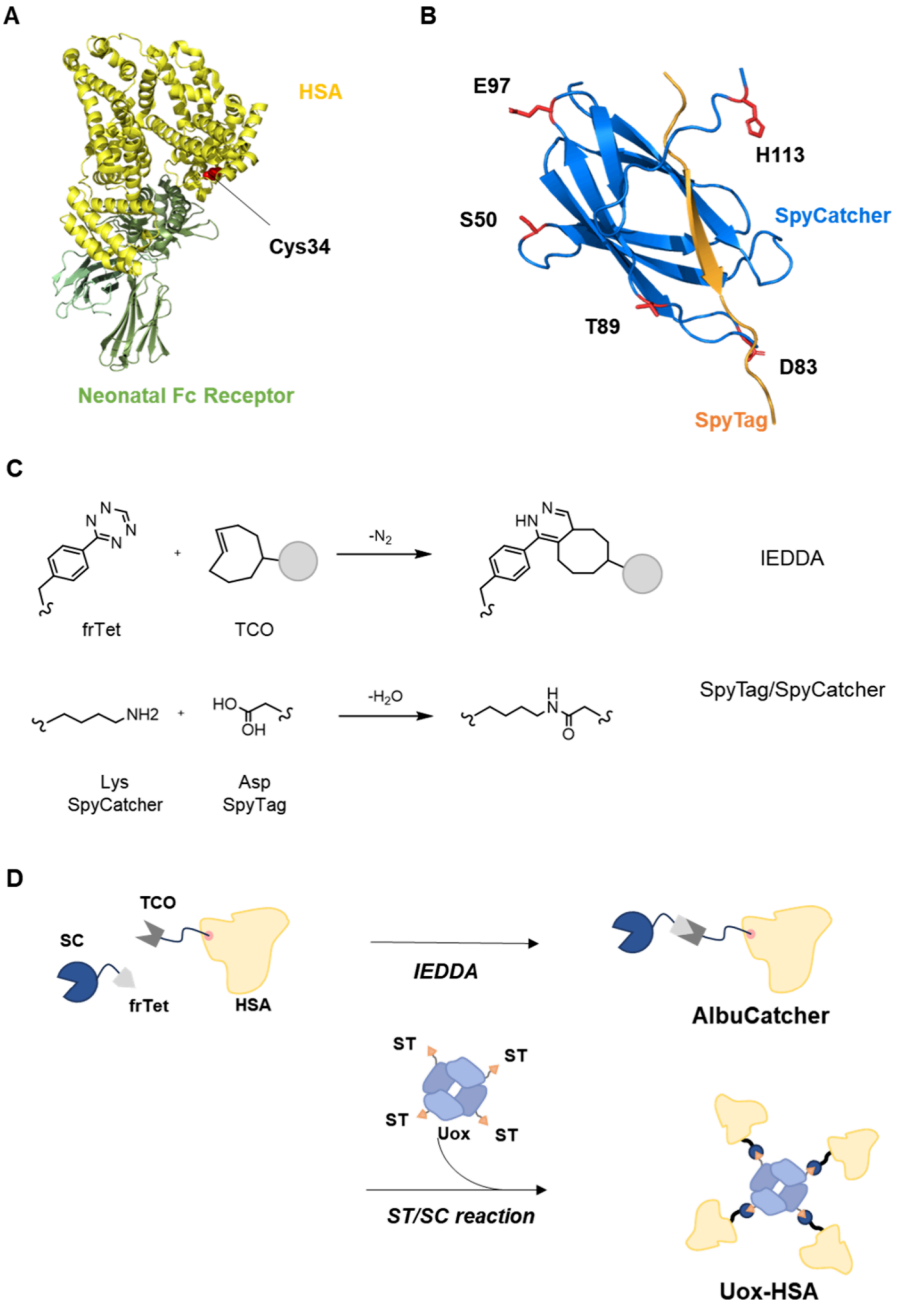

Figure 1. Schematic illustration showing (A) the interaction between HSA (yellow) and FcRn (green) (PDB ID: 4N0F) with the free cysteine at position 34 on HSA marked red, (B) the interaction between ST (orange) and SC (blue) with the side chains of the frTet incorporation sites (S50, D83, T89, E97, and H113) highlighted in red, (C) the reactions—inverse electron-demand Diels−Alder reaction (IEDDA) and SpyTag/SpyCatcher system (ST/SC)—and (D) the construction of AlbuCatcher and its reaction with ST-fused urate oxidase (Uox) to obtain HSA-conjugated Uox.

SC. We hypothesized that a simple mixing of AlbuCatcher with a therapeutic protein with a small ST would generate the therapeutic protein variant with a substantially enhanced serum half-life without compromising their activity. In other words, by preparing AlbuCatcher in advance, it is possible to enhance the pharmacokinetic properties of diverse therapeutic proteins with ST.

HSA conjugation to random sites on SC may reduce the activity of SC. Therefore, we employed site-specific HSA conjugation to a specific site on SC to minimize activity loss. For site-specific conjugation, we chose the inverse electron-demand Diels−Alder (IEDDA) reaction. Since the IEDDA reaction rate is much faster than other click chemistries such as copper-mediated azide−alkyne cycloaddition and strain-promoted azide−alkyne cycloaddition, the coupling efficiency between two macromolecules is high.[16] To utilize IEDDA, we first introduced a phenylalanine analogue containing tetrazine group (frTet) into a specific site of SC using the engineered *Methanococcus janacci* tyrosyl-tRNA/synthetase (MjtRNA^{Tyr}/MjTyrRS) pair[10,16,17] (Figure 1B). The conjugation site candidates were identified by evaluating the solvent accessibility and folding stability predicted by computational techniques. Subsequently, a heterobifunctional cross-linker featuring a trans-cyclooctene (TCO) and maleimide was

https://doi.org/10.1021/acsomega.4c02303
ACS Omega 2024, 9, 22990−23000

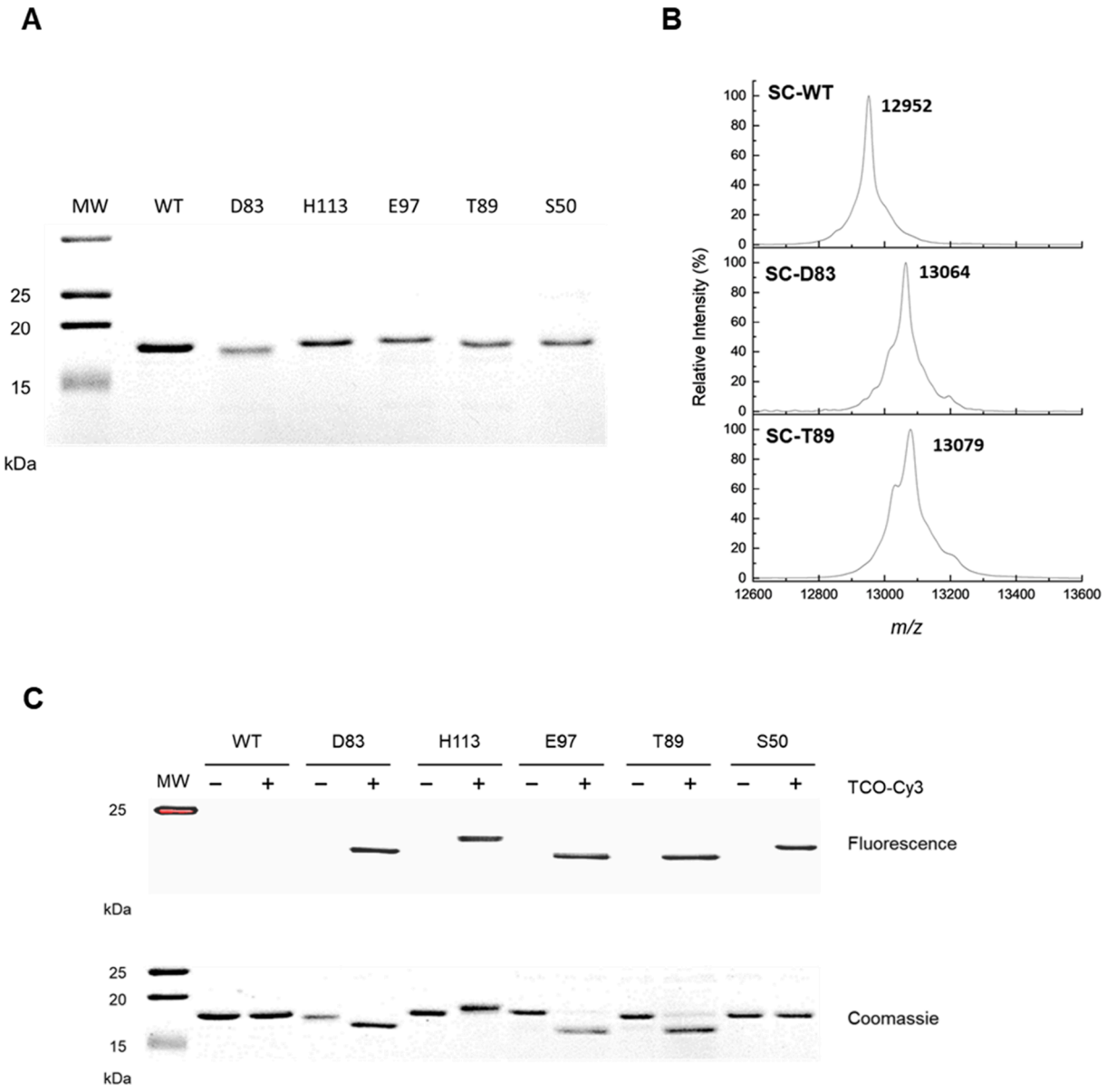

Figure 2. Preparation and characterization of SC variants (wild-type SC (WT), SC-D83 (D83), SC-H113 (H113), SC-E97 (E97), SC-T89 (T89), and SC-S50 (S50)). (A) Coomassie brilliant blue-stained protein gels of purified SC variants. Lane MW: molecular weight marker. (B) MALDI-TOF MS analysis of intact SC-WT, SCD83, and SC-T89. (C) Fluorescence analysis (illumination λex = 302 nm, with wavelengths at 510 to 610 nm in Chemidoc XRS + system) and Coomassie brilliant blue-stained protein gels of SC variants incubated with (+) or without (−) TCO-Cy3. Lane MW: molecular weight marker.

conjugated to the only free cysteine at position 34 (Cys34) of HSA to create an HSA linker intermediate. Next, the SC variant containing frTet (SC-frTet) was conjugated to the HSA linker intermediate to generate AlbuCatcher via IEDDA reaction (Figure 1C,D).

Urate oxidase (Uox), a tetrameric enzyme used in the treatment of gout, was chosen as the model protein in this study. Its primary function is to lower serum uric acid concentrations by catalyzing the conversion of insoluble uric acid to soluble 5-hydroxyisourate. Since Uox has a short half-life, extending the half-life has been critical for its clinical development.[12,18−20] ST was fused to Uox to generate Uox-ST. AlbuCatcher and Uox-ST were mixed to produce Uox-HSA via ST/SC reaction. The serum half-life of the final construct was assessed in vivo.

RESULTS AND DISCUSSION

Protein Design and Computation. Computational methods were employed in this study to screen for the optimal frTet incorporation site(s) in SC to ensure a high albumin conjugation yield while maintaining the SC/ST reaction capacity. An amino acid residue with higher solvent accessibility for the incorporation site of frTet increases the likelihood of collision with the TCO moiety, resulting in effective conjugation. Sites prone to perturbing the native structure upon frTet incorporation were excluded. Thus, the solvent accessibility, structural features, and computed stability of SC variants were considered. Since the crystal structure for the third-generation SC was not available, a predicted structure was generated by AlphaFold2.[21,22] Subsequently, the determination of the secondary structure and the solvent accessible

https://doi.org/10.1021/acsomega.4c02303
ACS Omega 2024, 9, 22990−23000

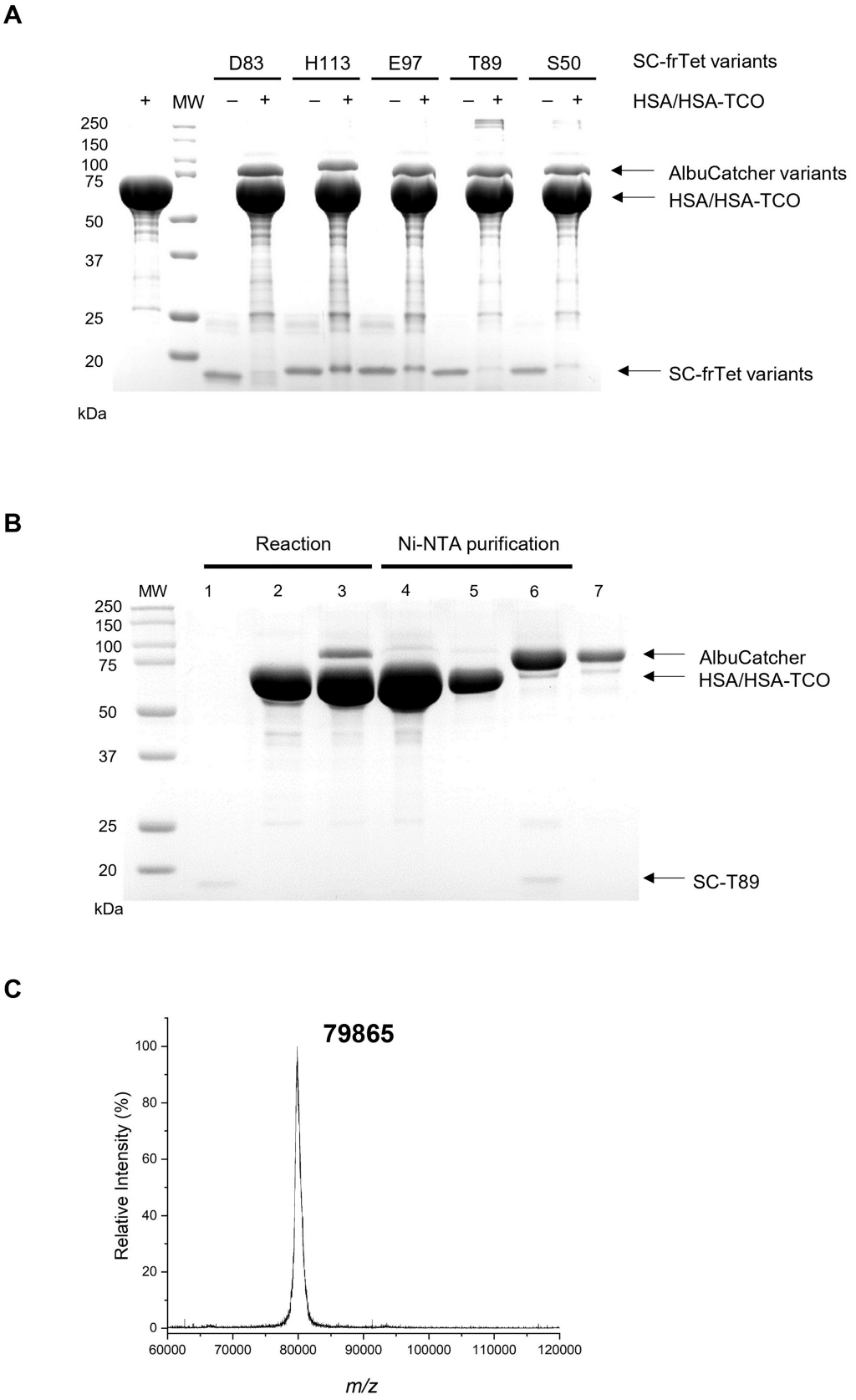

Figure 3. Preparation and characterization of AlbuCatcher. (A) SDS-PAGE analysis of the reaction mixture of SC-frTet variants in the absence (−) or presence (+) of HSA-TCO. (B) Protein gel of purification stained with Coomassie brilliant blue. Lane 1, SC-T89; Lane 2, HSA/HSA-TCO; Lane 3, reaction mixture; Lane 4, flow-through; Lane 5, washed solution; Lane 6, eluted solution; Lane 7, column-purified AlbuCatcher. (C) MALDI-TOF mass spectrum of AlbuCatcher.

https://doi.org/10.1021/acsomega.4c02303
ACS Omega 2024, 9, 22990−23000

surface area (SASA) of each residue was performed using PyMOL. Energy scores were calculated for a single mutation of each SC residue to either Y or W with PyRosetta[23] (Table S1).

Residues with a SASA value of 75 or higher and an energy score deviation of less than 5 compared with the wild type were selected. Additionally, residues involved in secondary structures and those parts of the hexahistidine tag (HisTag) for purification were excluded. To avoid interfering with the ST/SC association, the reactive residue (lysine at residue 32) and catalytic residue (glutamic acid at residue 78) were excluded. The residues that changed throughout the three-step evolution of the ST/SC system[13−15] were dismissed to maintain stability and fast reactivity. Furthermore, positions in close proximity to the N-terminal (residues 1−22) were disregarded, considering the studies regarding truncation of these residues to reduce immune response.[24,25] These criteria led to the identification of five candidate sites (aspartic acid at residue 83 (D83), histidine at residue 113 (H113), glutamic acid at residue 97 (E97), threonine at residue 89 (T89), and serine at residue 50 (S50)) for frTet incorporation (Figure 1C) (Table S2).

Site-Specific Incorporation of frTet into SC. Each of the five sites was successfully substituted to an amber codon (UAG) by polymerase chain reaction(PCR)-mediated site-directed mutagenesis. C321.ΔA.exp *E. coli* cells were cotransformed with pDule_C11RS plasmid encoding the engineered MjtRNA^{Tyr}/MjTyrRS pair as well as the plasmid encoding each SC-frTet variant gene. Five SC-frTet variants (SC-D83, SC-H113, SC-E97, SC-T89, and SC-S50) were expected to contain frTet at the D83, H113, E97, T89, and S50 site, respectively.

Those SC-frTet variants along with SC-WT were expressed as mentioned in the Materials and Methods section and then purified using metal-affinity chromatography. The production yields of SC-WT and SC-frTet variants (SC-D83, SC-H113, SC-E97, SC-T89, and SC-S50), evaluated in triplicates, were 18.5 ± 1.1, 6.7 ± 1.3, 4.8 ± 0.3, 5.8 ± 0.2, 5.7 ± 0.2, and 4.4 ± 0.9 mg/L, respectively. The production yields of SC-frTet variants were 3 to 4 times smaller than that of SC-WT, most likely because the amber codon suppression is usually incomplete leading to translational termination without incorporation of frTet.[26]

Each purified SC-frTet variant exhibited a single dominant band between 15 and 20 kDa (Figure 2A) in the protein gel, suggesting that the expression and purification of SC-frTet were successful. Since the expected mass of SC variants is about 13 kDa, we performed the MALDI-TOF analysis to further confirm the identity of purified proteins. As representative cases, we analyzed intact SC-WT, SC-D83, and SC-T89 (Figure 2B). The experimentally determined masses of SC-WT, SC-D83, and SC-T89 were 12,952, 13,064, and 13,079 m/z, respectively, which were quite comparable to the expected values of 13,080, 13,192, and 13,206 m/z each within a deviation of 1%. However, there is an intrinsic inaccuracy in the determination of absolute values of intact protein mass by MALDI-TOF, because the average masses are considered instead of monoisotopic masses and the calibration may not be entirely accurate. Therefore, we also analyzed mass differences among the samples. The substitutions of aspartic acid and threonine with frTet were expected to show a difference of 112 and 126 m/z, respectively. The observed shifts of 112 m/z and 127 m/z were closely in agreement with these expectations

The fluorescent dye labeling of intact SC-frTet variants was carried out to validate the reactivity of incorporated frTet. SC-frTet variants were incubated with or without TCO-Cy3 and analyzed using sodium dodecyl sulfate-polyacrylamide gel electrophoresis (SDS-PAGE). The protein gel stained with Coomassie brilliant blue (CBB) showed prominent bands across all variants (Figure 2C). When examined under fluorescence imaging, the SC-WT did not display any fluorescence. In contrast, SC-frTet variants exhibited substantial fluorescence upon dye conjugation (Figure 2C). Faint bands in the positions corresponding to unreacted SC are present in SC-E97 and SC-T89. We speculate that these are likely due to an incomplete reaction with TCO-Cy3. The TCO-Cy3 conjugation yield is defined as the amount of the Cy3-conjugated SC-variant divided by the amount of SC-variant (percentage). The yields for SC-E97 and SC-T89 were 94% and 91%, respectively. Overall, these results demonstrated the successful preparation of SC-WT and SC-frTet variants with IEDDA reactivity.

Site-Specific HSA Conjugation to Generate AlbuCatcher. To select the site with the highest conjugation yield, SC-frTet variants were conjugated to HSA using a heterobifunctional cross-linker, *Trans*-cyclooctene-PEG4-maleimide (TCO-PEG4-MAL). TCO functionality was introduced to HSA (HSA-TCO) by attaching TCO-PEG4-MAL to the free cysteine at residue 34 (C34) through a thiol-maleimide reaction. C34 has been readily used for conjugation due to its location away from the FcRn-binding domain.[27] Previous studies have demonstrated that (therapeutic) proteins conjugated to C34 did not compromise the ability of HSA to bind to FcRn, thereby extending serum half-life.[9,10,17] Site-specific conjugation of SC to HSA through IEDDA was performed by mixing each SC-frTet variant with HSA-TCO, generating the SC-HSA conjugate (AlbuCatcher). The reaction mixture in the absence and presence of HSA-TCO was subjected to SDS-PAGE analysis and the band intensities were compared upon CBB-staining (Figure 3A). Among the five variants tested, SC-T89 exhibited the highest conjugation yield of 91%, followed by those of SC-D83 (89%), SC-S50 (83%), SC-E97 (60%), and SC-H113 (43%).

The AlbuCatcher variant produced from the conjugation between HSA-TCO and SC-T89 was further purified via a two-step purification method. The affinity between HisTag and Ni-nitrilotriacetic acid (Ni-NTA) agarose gels resulted in a mixture of AlbuCatcher and free SC-T89, which has a HisTag (Figure 3B; Lane 6). In contrast, most HSA-TCO was removed as it lacked affinity toward Ni-NTA (Figure 3B; Lanes 4, 5). Further purification by SEC was necessary as SC-T89 can interfere when reacting AlbuCatcher and a therapeutic protein harboring ST. The purified AlbuCatcher was subjected to MALDI-TOF MS analysis. The spectrum of AlbuCatcher showed a mass peak at 79,865 m/z, corresponding well with the expected value (79,975 m/z) with less than 0.2% deviation (Figure 3C). Hence, AlbuCatcher was prepared in high purity (>90%).

Preparation and Characterization of Uox Variants. Uox was chosen as the therapeutic protein to be conjugated with HSA, as mediated by the ST/SC reaction. Therefore, Uox-ST was generated by appending the 16 amino acid sequence (RGVPHIVMVDAYKRYK) of ST to the C-terminus of wild-type UOX (Uox-WT), utilizing a flexible $(GGS)_6$ linker. Uox-WT and Uox-ST were produced using bacterial expression systems and purified through metal-affinity

https://doi.org/10.1021/acsomega.4c02303
ACS Omega 2024, 9, 22990−23000

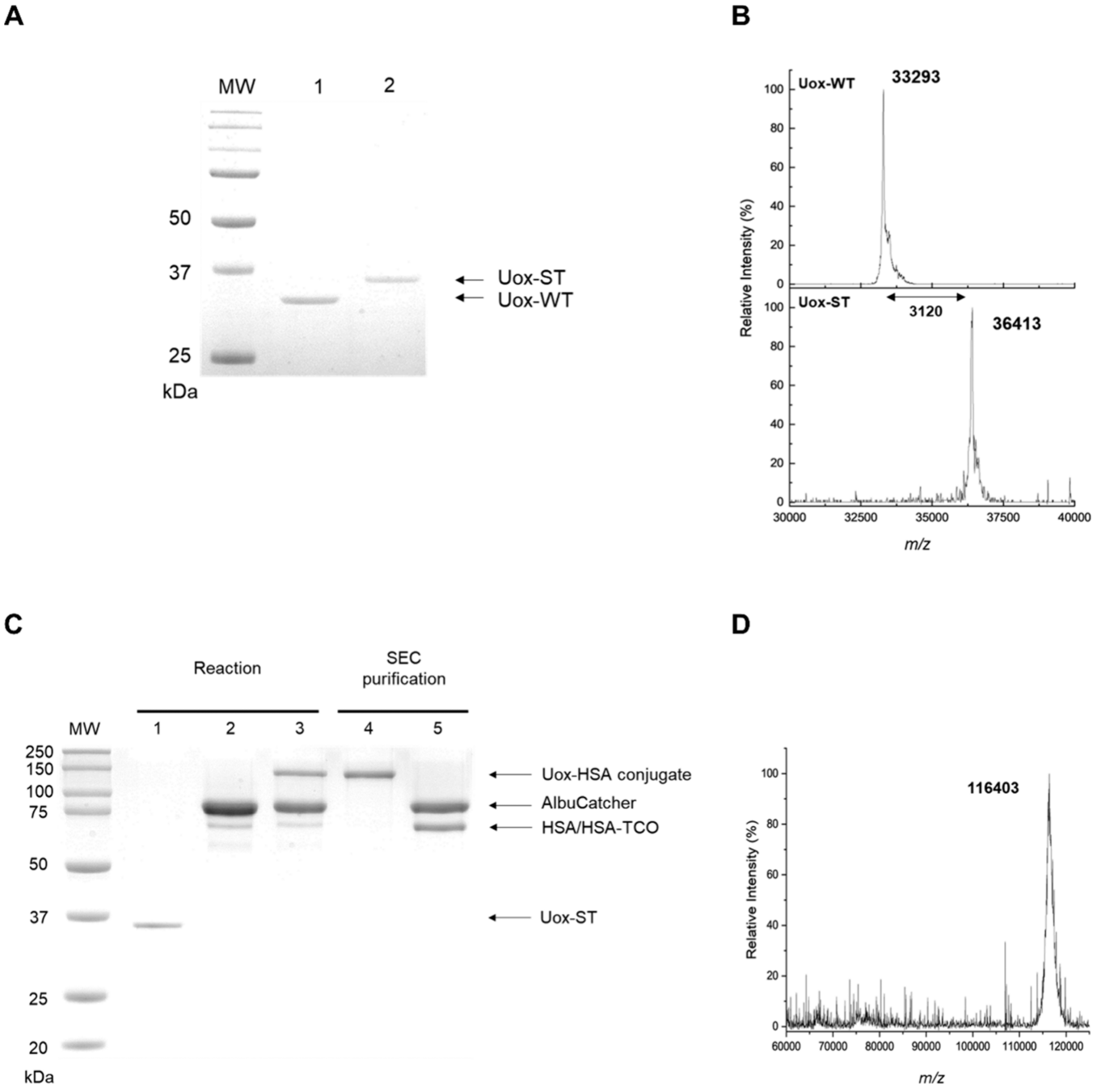

Figure 4. Purification and characterization of Uox species (Uox-WT, Uox-ST, and Uox-HSA). (A) Coomassie brilliant blue-stained protein gel: Lane 1, Uox-WT; Lane 2, Uox-ST. (B) MALDI-TOF analyses of Uox-WT and Uox-ST. (C) The generation and purification of the Uox-HSA conjugate: Lane 1, Uox-ST; Lane 2, AlbuCatcher, Lane 3, reaction mixture; Lane 4, column-purified Uox-HSA; Lane 5, residual AlbuCatcher. (D) MALDI-TOF MS of the Uox-HSA conjugate.

chromatography. The production yield of Uox-ST (37.1 ± 1.3 mg/L) was comparable to that of Uox-WT (54.3 ± 1.0 mg/L). The SDS-PAGE analysis of Uox-WT and Uox-ST gave bands between 25 kDa and 37 kDa molecular weight standards, corresponding well to the expected molecular weight of monomeric Uox-WT (about 33.5 kDa) and Uox-ST (about 36.5 kDa), respectively (Figure 4A). This was attributable to the dissociation of the homotetramer complex into single units upon exposure to SDS during SDS-PAGE analysis. Notably, the Uox-ST band exhibited an upward shift relative to that of Uox-WT, implying the insertion of ST.

Further analysis using MALDI-TOF mass spectrometry showed the intact masses of 33,293 m/z for Uox-WT and 36,413 m/z for Uox-ST agreeing closely with the expected values (Uox-WT:33,455 m/z; Uox-ST:36,577 m/z) with a deviation less than 0.5% (Figure 3B). In addition, the measured mass difference (3,120 m/z) matched well with the expected contribution of the inserted linker and ST (3,121 m/z). These results demonstrated the successful preparation of Uox-WT and Uox-ST.

SC/ST Reaction to Generate Uox-HSA. To achieve the conjugation of Uox with HSA, the spontaneous coupling between the ST and SC was utilized. The reactivity of SC-T89

https://doi.org/10.1021/acsomega.4c02303
ACS Omega 2024, 9, 22990−23000

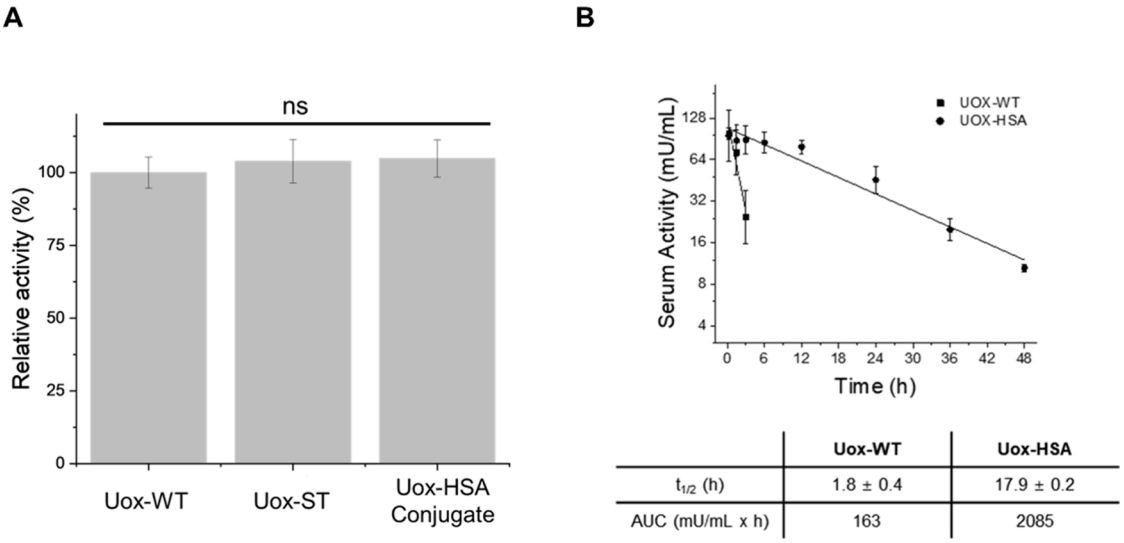

	Uox-WT	Uox-HSA
$t_{1/2}$ (h)	1.8 ± 0.4	17.9 ± 0.2
AUC (mU/mL x h)	163	2085

Figure 5. Enzymatic assay of Uox variants in vitro and in vivo. (A) The relative enzymatic activity of the Uox species. The relative enzymatic activities were normalized to the enzymatic activity of Uox-WT. Experiments were performed in triplets, and error bars mean standard deviations. The data were subjected to one-way ANOVA with Tukey's posthoc test, and "ns" means there is no significant difference. (B) Pharmacokinetic studies of Uox-WT and Uox-HSA conjugate in mice (n = 5). Samples were intravenously injected into BALB/c female mice. The remaining enzymatic activity of the residual Uox variants were measured at different time points: 0.25, 1.5, and 3 h for Uox-WT; 0.25, 1.5, 3, 6, 12, 24, 36, and 48 h for Uox-HSA conjugate.

was comparable to that of the wild type (Figure S1). Uox-ST and AlbuCatcher were prepared in advance and reacted by mixing them together. SDS-PAGE analysis revealed a monomeric Uox-HSA conjugate band between 100 and 150 kDa in the reaction mixture (Figure 4C, Lane 3). The absence of Uox-ST monomer in the mixture for conjugation (Figure 4C, Lane 3), indicated an almost complete reaction between Uox-ST and AlbuCatcher. Subsequently, Uox-HSA and the remaining AlbuCatcher were separated using SEC (Figure 4C, Lanes 4 and 5). To further confirm the conjugation of Uox-ST and AlbuCatcher, we performed the MALDI-TOF MS analysis of the Uox-HSA conjugate. A peak of 116,403 m/z was observed, corresponding to the expected value, 116,515 m/z, within a deviation of 0.1% (Figure 4D). Overall, the successful conjugation of Uox-ST and AlbuCatcher through ST/SC chemistry was demonstrated.

In Vitro Enzyme Assay of Uox Variants. The impact of ST fusion or HSA conjugation on the enzymatic activity of Uox was investigated by comparing uric acid degradation of Uox-WT, Uox-ST, and Uox-HSA conjugates in PBS (pH 7.4) at 37 °C to emulate physiological conditions. The enzymatic activities of all variants were comparable, suggesting that neither fusion nor conjugation significantly reduces the enzymatic activity of Uox (Figure 5A).

Pharmacokinetics Study of Uox-WT and Uox-HSA Conjugate in Vivo. To evaluate the pharmacokinetic effects of Uox conjugated with HSA via the ST/SC reaction, we determined the serum half-lives of the Uox-WT and Uox-HSA conjugate after intravenous injection in BALB/c mice (n = 5). We collected the serum samples at predetermined time points (0.25, 1.5, and 3 h for Uox-WT and 0.25, 1.5, 3, 6, 12, 24, 36, and 48 h for Uox-HSA). Subsequently, we performed enzymatic activity assays to determine the serum half-lives of the Uox-WT and Uox-HSA conjugates. We observed that the serum half-life of Uox-WT was 1.8 ± 0.4 h, which was consistent with the previously reported values (Figure 5B).[10,28] However, the serum half-life of the Uox-HSA conjugate was significantly longer at 17.9 ± 0.2 h, which is approximately 10 times longer when compared to Uox-WT (Figure 5B). Moreover, the Uox-HSA conjugate showed an approximately 12.77-fold increase in the AUC values, which were calculated to be 163 and 2085 for the Uox-WT and Uox-HSA conjugates, respectively (Figure 5B). These results demonstrate a significant increase in the half-life of Uox following the conjugation of HSA via ST/SC reaction. A correlation between the apparent FcRn-binding affinity and in vivo half-life extension has been previously reported.[16] In addition, when the molecular weight of a macromolecule exceeded the renal filtration threshold (about 70 kDa), no substantial difference in kidney elimination was observed.[29] Therefore, the prolonged serum half-life was speculated to be predominantly attributed to FcRn-mediated recycling of HSA, given that the molecular weight of unmodified tetrameric Uox (about 134 kDa) surpasses the renal filtration threshold. Furthermore, since HSA is known to have a substantially lower binding affinity for mFcRn compared to the binding between human FcRn and HSA,[30] it is highly likely that the FcRn-mediated recycling of HSA-conjugated Uox will be even more effective in higher animal models.

MATERIALS AND METHODS

Materials. *Eco*RI and *Hind*III were purchased from New England Biolabs (Ipswich, MA, USA). In-Fusion HD Enzyme Premix was obtained from Takara Bio (Kusatsu, Japan). Yeast extract and tryptone were bought from DB Biosciences (San Jose, CA, USA). L-(+)-Arabinose, isopropyl-β-D-thiogalacto-pyranoside (IPTG), and Zeba spin desalting columns (MWCO 7 kDa) were purchased from Thermo Fisher Scientific (Waltham, MA, USA). frTet [4-(1,2,4,5-tetrazin-3-yl) phenylalanine] was obtained from WuXi Apptech (Shanghai, China). TCO-PEG4-MAL was bought from Futurechem (Seoul, Korea). TCO-Cy3 was purchased from AAT Bioquest (Sunnyvale, CA). Desalting columns (PD-10), the anion exchange column (HiTrap Q HP, 5 mL), and the

https://doi.org/10.1021/acsomega.4c02303
ACS Omega 2024, 9, 22990−23000

size exclusion column (Superdex 200 10/300 Gl Increase) were purchased from Cytiva (Uppsala, Sweden). Ni-NTA and polypropylene columns were obtained from Qiagen (Hilden, Germany). Vivaspin 6 columns (MWCO 10 kDa) were sourced from Sartorius (Göttingen, Germany). A steel target plate, α-cyano-4-hydroxycinnamic acid, and Protein Standard I, II were purchased from Bruker (Billerica, MA, USA). Trifluoroacetic acid (99%) was bought from Daejung Chemicals & Metals (Gyeonggi, Korea). Immunoplates (96-well, flat) were obtained from SPL Life Sciences (Gyeonggi, Korea). All other reagents were purchased from Sigma-Aldrich (St. Louis, MO, USA) unless otherwise specified.

Computational Analysis of the frTet Incorporation Site in SC. Computational screening was employed to identify permissive frTet incorporation sites in SC. This method was developed based on the successful selection of frTet incorporation sites utilizing energy scores calculated by PyRosetta, as previously reported.[10] Structure analysis was performed using PyMOL Version 2.4.1 (Schrödinger, New York, NY, USA) and PyRosetta (Python-based Rosetta molecular modeling package; Pyrosetta4) based on the model generated with ColabFold, a web server offering protein structure prediction by combining fast homology search with AlphaFold2. Parameters such as the solvent accessible surface area (SASA) and residues forming secondary structures (α-helix, β-sheet, or random coil) were determined with PyMOL. Energy scores were calculated by the energy score function provided by PyRosetta following the substitution of each residue with either tyrosine (Y) or tryptophan (W).

Construction of Plasmids. The gene for SC-WT was amplified from SpyCatcher003-sfGFP (Addgene plasmid #133449) using primers (F: 5′-GCAT GAATTC ATTAAAG-AGGAGAAATTA ATGGTAACCACCTTATCAGGTTTAT-CAG-3′, R: 5′-CGTAAAGCTT TCAAGTATGAGCGTCAC-CTTCAGT-3′). The DNA fragment was inserted into pQE80_Uox[10] using the restriction enzymes *Eco*RI and *Hind*III. The deletion of the unnecessary gene and the insertion of a hexahistidine site was performed by in-fusion cloning using primers (F: 5′- CACCATCACCATTAATA-ATGAGAGCTCGGTACCCCGG-3′, R: 5′- TTAATGG-TGATGGTGATGGTGAGTATGAGCGTCACCTTCA-GTTGC-3′). In-Fusion HD Enzyme Premix was mixed with the PCR product to finalize the generation of pQE80_SC-WT. The vector was linearized by PCR using primers (F: 5′-TAAAGCTCGAGATCTGCAGCTGG-3′, R: 5′-GGTTAA-TTCCTCCTGTTAGCCCAAAAAACG-3′) with pBAD_sfGFP[17] as a template, and SC-WT with hexahistidine tag (HisTag) was amplified with primers (F: 5′-CAGGAG-GAATTAACCATGGTAACCACCTTATCAGGTTTATC-3′, R: 5′-AGATCTCGAGCTTTATTAATGGTGATGGTG-ATGGTGAG-3′) using pQE80_SC-WT described above as a template. The two PCR products were mixed with 5X In-Fusion HD Enzyme Premix to generate pBAD_SC-WT. Each of the sites selected by computational methods was replaced with an amber codon (UAG) by site-directed mutagenesis (PCR) using pBAD_SC-WT as a template. The primer pairs used are shown in Table S3.

In-fusion cloning was performed to generate pQE80_Uox-ST using pQE80_Uox-ABD[31] as a template. Linearized Uox-ST with a hexahistidine tag was amplified by PCR with primers (F: 5′-TTGTTATGGTGGACGCCTACAAACGCTATA-AACACCATCACCATCACCATTAAGC-3′, R: 5′-GTC-CACCATAACAATATGAGGAACGCCACGGCTGCC-ACCAGAACCAC-3′). The PCR product was mixed with the In-Fusion HD Enzyme Premix to generate pQE80_Uox-ST.

Expression and Purification of SC Variants and Uox Variants. Site-specific incorporation of frTet into SC was performed by cotransforming pDule_C11RS plasmid and the plasmid harboring the gene encoding each SC variant into C321.ΔA.exp host cells. Precultured cells were inoculated in 2xYT containing 100 μg/mL ampicillin and 10 μg/mL tetracycline and then vigorously shaken at 200 rpm, 37 °C. For the expression of SC-frTet variants, 1 mM frTet and 0.4% arabinose were added when the optical density at 600 nm (OD_{600}) reached 0.4 and 0.6, respectively. Afterward, the cells were incubated at 18 °C for 24 h. For the preparation of SC-WT, the pQE80_SC-WT plasmid was transformed into chemically competent BL21 *E. coli* cells. Overnight cultures were inoculated in 2xYT containing 100 μg/mL ampicillin and induced with 1 mM IPTG at OD_{600} 0.6. The cells were cultured at 37 °C for 6 h. To express the Uox variants, the plasmids encoding pQE80_Uox-WT[10] and pQE80_Uox-ST were separately transformed into chemically competent BL21 *E. coli* cells. Precultured cells were inoculated in fresh 2xYT with 100 μg/mL ampicillin, and induction was initiated with 1 mM IPTG when OD_{600} reached 0.6. Uox-WT was incubated for 6 h under the same conditions, while Uox-ST was incubated for 16 h after lowering the temperature to 18 °C.

The cultured cells were pelleted by centrifugation at 6000 rpm for 10 min and stored at −80 °C until further use. Cells resuspended in the lysis buffer (50 mM NaH_2PO_4, 300 mM NaCl, and 10 mM imidazole, pH 8.0) were sonicated for cell lysis. The clear supernatant, recovered after centrifugation at 12,000 rpm for 20 min, was mixed by rotation with Ni-NTA agarose at 4 °C for 1 h. Using a gravity-flow polypropylene column, the mixture was washed with washing buffer (50 mM NaH_2PO_4, 300 mM NaCl, 20 mM imidazole, pH 8.0) to remove impurities. Proteins were eluted by elution buffer (50 mM NaH_2PO_4, 300 mM NaCl, 250 mM imidazole, pH 8.0), and then the buffer was exchanged with PBS (pH 7.4) on PD-10 desalting columns according to the manufacturer's protocol (Cytiva).

Matrix-Assisted Laser Desorption Ionization Time-of-Flight Mass Spectrometry (MALDI-TOF MS). Intact SC variants were desalted by Zebaspin (7K-MWCO) and applied as a single layer after being mixed with an HCCA matrix containing α-cyano-4-hydroxycinnamic acid saturated in TA30 (30% acetonitrile, 0.1% trifluoroacetic acid in water) at a 1:1 ratio. Similarly, intact proteins (Uox-WT, Uox-ST, Albu-Catcher, and Uox-HSA) were prepared. They were mixed with an equal volume of sinapinic acid (SA) matrix solution II (SA saturated in TA30) and then applied onto a predeposited layer of SA matrix solution I (SA saturated in ethanol) instead.

Next, the samples were transferred onto a steel plate target and air-dried before acquiring mass spectra using an Autoflex MALDI-TOF instrument (Bruker Corporation, Billerica, MA, USA). Calibration was conducted using protein standard I (4−20 kDa) for SC variants and protein standard II (20−90 kDa) for the rest of the reaction before measurement.

Dye Labeling Analysis of SC Variants. Purified SC-frTet variants were separately incubated with TCO-Cy3 dye at a molar ratio of 1:2 in PBS (pH 7.4) for 2 h at RT. The samples with or without TCO-Cy3 were loaded onto SDS-PAGE gels to measure the in-gel fluorescence using a ChemiDoc XRS+ System (Bio-Rad Laboratories, Hercules, CA, USA), with emitted light between 510 and 610 nm being detected upon

https://doi.org/10.1021/acsomega.4c02303
ACS Omega 2024, 9, 22990−23000

excitation at 302 nm. Further visualization involved the CBB-staining of the protein gel.

Generation of AlbuCatcher and Uox-HSA Conjugate. Lyophilized HSA was dissolved in 20 mM BisTris buffer (pH 7.0), and high molecular impurities were removed through anion exchange chromatography as previously reported.[8,10] The purified HSA was reacted with a TCO-PEG4-MAL heterobifunctional cross-linker at a molar ratio of 1:4 for 2 h at room temperature. Unreacted cross-linkers were desalted on a PD-10 column with PBS (pH 7.4). Subsequently, SC-frTet variants were mixed with HSA-TCO at a molar ratio of 1:4 for 6 h at room temperature to generate AlbuCatcher variants and analyzed by SDS-PAGE to identify the site-specific albumin conjugation yield visualized by CBB-staining. The purification of AlbuCatcher was carried out by incubating the reaction mixture with Ni-NTA at 4 °C for 1 h. Unreacted HSA-TCO was washed, and AlbuCatcher was eluted as described above. Eluted protein was desalted using PD-10 with PBS (pH 7.4) and then loaded for size exclusion chromatography (SEC) using the NGC Quest 10 Plus Chromatography System (Biorad Laboratories Inc., Berkely, CA, USA). Purified Uox-ST and AlbuCatcher were mixed in a 1:4 molar ratio and incubated for 6 h at room temperature. The whole reaction mixture was loaded for SEC to remove the residual AlbuCatcher. The reaction and purification samples were analyzed with SDS-PAGE. The protein concentration was calculated based on the Beer−Lambert law using the molar extinction coefficients at 280 nm (ε_{280}).[32] The molar extinction coefficients, determined by the equation $\varepsilon_{280} = (5500 \times n_{Tryptophan}) + (1490 \times n_{Tyrosine}) + (125 \times n_{Disulfide\ bond}) + (9{,}600 \times n_{frTet})$, are listed in the Table S4.

Enzyme Activity Assay of Uox variants. The enzyme activities of Uox species (Uox-WT, Uox-ST, and Uox-HSA) were measured by the uric acid degradation assay as described previously with slight modifications.[33,34] The reaction was carried out at 37 °C, where 60 nM Uox species was incubated with 200 μM of uric acid in 200 μL of PBS (pH 7.4). The degradation of uric acid was then monitored by measuring the change in the optical density at 293 nm.

Pharmacokinetics Study of Uox-WT and Uox-HSA Conjugate in Vivo. The pharmacokinetic study of the Uox-WT and Uox-HSA conjugate was conducted following the guidelines of the Animal Care and Use Committee at the Gwangju Institute of Science and Technology (GIST-2021-092). Uox-WT and Uox-HSA conjugate (1.74 nmol based on Uox monomer in 200 μL of PBS at pH 7.4) were injected into the tail vein of 7-week-old female BALB/c mice (n = 5). Blood samples were collected via retro-orbital bleeding at specific time points (0.25, 1.5, and 3 h for Uox-WT and 0.25, 1.5, 3, 6, 12, 24, 36, and 48 h for Uox-HSA conjugate). After blood collection, serum was separated from the blood through centrifugation at 1,500 g at 4 °C for 10 min and stored at −20 °C for subsequent use. Following separation of the serum from the blood, the serum activity of Uox was determined using the uric acid degradation rate. In brief, the serum was mixed with an enzymatic activity assay buffer (50 mM sodium borate, pH 9.5) containing 200 μM uric acid at a 1:8 ratio in a 96-well plate. The absorbance change at 293 nm was measured, and serum activity (mU/mL) was calculated over time using the extinction coefficient value of uric acid (123,000 $L \cdot mmol^{-1} \cdot cm^{-1}$).

CONCLUSION

In this study, we addressed the challenges associated with enhancing the serum half-life of therapeutic proteins, focusing on the development of a novel technology named AlbuCatcher. By leveraging the ST/SC system, we successfully conjugated HSA to a therapeutic protein, exemplified here by Uox. To prepare site-specifically HSA conjugated SC, we employed IEDDA reaction, utilizing frTet introduced into a specific site of SC. Computational methods were employed to identify optimal frTet incorporation sites, considering solvent accessibility, structural features, and computed stability of the SpyCatcher variants. The subsequent conjugation of HSA to SC via IEDDA reaction yielded AlbuCatcher with high purity (>90%). The Uox-ST variant, generated by fusing ST to Uox, was successfully conjugated with AlbuCatcher via the ST/SC reaction. Importantly, the in vitro enzyme assay confirmed that the enzymatic activity of the Uox-HSA conjugate was comparable to that of the unconjugated Uox-WT, indicating that the conjugation process did not compromise the therapeutic functionality of the protein. In vivo pharmacokinetic studies in BALB/c mice revealed a significant improvement in the serum half-life of Uox-HSA compared to Uox-WT. These findings underscore the efficacy of AlbuCatcher in enhancing the pharmacokinetics of therapeutic proteins, paving the way for the development of long-acting biopharmaceuticals.

In conclusion, the strategy employing AlbuCatcher, based on the ST/SC system, offers a promising strategy for extending the serum half-life of therapeutic proteins, addressing key challenges associated with other conjugation methods. The high reactivity of AlbuCatcher can be utilized for extending the serum half-life of various therapeutic proteins, whether monomeric or multimeric, through reduced renal filtration via size extension and FcRn-mediated recycling. The success of the Uox-HSA conjugate in achieving prolonged circulation highlights the potential of AlbuCatcher in advancing the field of biopharmaceuticals and improving the therapeutic outcomes of protein-based drugs.

ASSOCIATED CONTENT

Supporting Information

The Supporting Information is available free of charge at https://pubs.acs.org/doi/10.1021/acsomega.4c02303.

> Amino acid mutation scoring, solvent accessibility of SpyCatcher; full sequence of proteins; primer pairs used for PCR-mediated SDM of SC; extinction coefficients at 280 nm for protein quantification; reaction of Uox-ST and SC variants (SC-WT, SC-D83, and SC-T89); and purification of AlbuCatcher and Uox-HSA conjugate (PDF)

AUTHOR INFORMATION

Corresponding Author

Inchan Kwon − *School of Materials Science and Engineering, Gwangju Institute of Science and Technology (GIST), Gwangju 61005, Republic of Korea;* orcid.org/0000-0003-0806-4116; Phone: +82 62-715-2312; Email: inchan@gist.ac.kr; Fax: +82 62-715-2304

https://doi.org/10.1021/acsomega.4c02303
ACS Omega 2024, 9, 22990−23000

Authors

Ji Hyun Rho − *School of Materials Science and Engineering, Gwangju Institute of Science and Technology (GIST), Gwangju 61005, Republic of Korea*

Jae Hun Lee − *School of Materials Science and Engineering, Gwangju Institute of Science and Technology (GIST), Gwangju 61005, Republic of Korea*

Complete contact information is available at: https://pubs.acs.org/10.1021/acsomega.4c02303

Notes

The authors declare no competing financial interest.

■ ACKNOWLEDGMENTS

This work was supported by GIST-CNUH research Collaboration grant funded by the GIST in 2024. The funder was not involved in the design of the study and collection, analysis, and interpretation of data and in writing the manuscript.

■ REFERENCES

(1) Mitragotri, S.; Burke, P. A.; Langer, R. Overcoming the Challenges in Administering Biopharmaceuticals: Formulation and Delivery Strategies. *Nat. Rev. Drug Discovery* **2014**, *13* (9), 655−672.

(2) Kontermann, R. E. Strategies for Extended Serum Half-Life of Protein Therapeutics. *Curr. Opin. Biotechnol.* **2011**, *22*, 868−876.

(3) Kratz, F. Albumin as a Drug Carrier: Design of Prodrugs, Drug Conjugates and Nanoparticles. *J. Controlled Release* **2008**, *132* (3), 171−183.

(4) Pyzik, M.; Sand, K. M. K.; Hubbard, J. J.; Andersen, J. T.; Sandlie, I.; Blumberg, R. S. The Neonatal Fc Receptor (FcRn): A Misnomer? *Frontiers in Immunology* **2019**, DOI: 10.3389/fimmu.2019.01540.

(5) Duttaroy, A.; Kanakaraj, P.; Osborn, B. L.; Schneider, H.; Pickeral, O. K.; Chen, C.; Zhang, G.; Kaithamana, S.; Singh, M.; Schulingkamp, R.; Crossan, D.; Bock, J.; Kaufman, T. E.; Reavey, P.; Carey-Barber, M.; Krishnan, S. R.; Garcia, A.; Murphy, K.; Siskind, J. K.; McLean, M. A.; Cheng, S.; Ruben, S.; Birse, C. E.; Blondel, O. Development of a Long-Acting Insulin Analog Using Albumin Fusion Technology. *Diabetes* **2005**, *54* (1), 251−258.

(6) Ikuta, S.; Chuang, V. T. G.; Ishima, Y.; Nakajou, K.; Furukawa, M.; Watanabe, H.; Maruyama, T.; Otagiri, M. Albumin Fusion of Thioredoxin — The Production and Evaluation of Its Biological Activity for Potential Therapeutic Applications. *J. Controlled Release* **2010**, *147* (1), 17−23.

(7) Kim, Y.-M.; Lee, S. M.; Chung, H.-S. Novel AGLP-1 Albumin Fusion Protein as a Long-Lasting Agent for Type 2 Diabetes. *BMB Reports* **2013**, *46* (12), 606−610.

(8) Lim, S. I.; Hahn, Y. S.; Kwon, I. Site-Specific Albumination of a Therapeutic Protein with Multi-Subunit to Prolong Activity in Vivo. *J. Controlled Release* **2015**, *207*, 93−100.

(9) Bak, M.; Park, J.; Min, K.; Cho, J.; Seong, J.; Hahn, Y. S.; Tae, G.; Kwon, I. Recombinant Peptide Production Platform Coupled with Site-Specific Albumin Conjugation Enables a Convenient Production of Long-Acting Therapeutic Peptide. *Pharmaceutics* **2020**, *12* (4), 364.

(10) Yang, B.; Kwon, I. Thermostable and Long-Circulating Albumin-Conjugated Arthrobacter Globiformis Urate Oxidase. *Pharmaceutics* **2021**, *13* (8), 1298.

(11) Podobnik, B.; Helk, B.; Smilović, V.; Škrajnar, Š.; Fidler, K.; Jevševar, S.; Godwin, A.; Williams, P. Conjugation of PolyPEG to Interferon Alpha Extends Serum Half-Life While Maintaining Low Viscosity of the Conjugate. *Bioconjugate Chem.* **2015**, *26* (3), 452−459.

(12) da Silva Freitas, D.; Spencer, P. J.; Vassão, R. C.; Abrahão-Neto, J. Biochemical and Biopharmaceutical Properties of PEGylated Uricase. *Int. J. Pharm.* **2010**, *387* (1−2), 215−222.

(13) Zakeri, B.; Fierer, J. O.; Celik, E.; Chittock, E. C.; Schwarz-Linek, U.; Moy, V. T.; Howarth, M. Peptide Tag Forming a Rapid Covalent Bond to a Protein, through Engineering a Bacterial Adhesin. *Proc. Natl. Acad. Sci. U. S. A.* **2012**, *109* (12), No. E690-E697.

(14) Keeble, A. H.; Banerjee, A.; Ferla, M. P.; Reddington, S. C.; Anuar, I. N. A. K.; Howarth, M. Evolving Accelerated Amidation by SpyTag/SpyCatcher to Analyze Membrane Dynamics. *Angew. Chem.* **2017**, *129* (52), 16748−16752.

(15) Keeble, A. H.; Turkki, P.; Stokes, S.; Khairil Anuar, I. N. A.; Rahikainen, R.; Hytönen, V. P.; Howarth, M. Approaching Infinite Affinity through Engineering of Peptide-Protein Interaction. *Proc. Natl. Acad. Sci. U. S. A.* **2019**, *116* (52), 26523−26533.

(16) Yang, B.; Kwon, I. Multivalent Albumin-Neonatal Fc Receptor Interactions Mediate a Prominent Extension of the Serum Half-Life of a Therapeutic Protein. *Mol. Pharmaceutics* **2021**, *18* (6), 2397−2405.

(17) Yang, B.; Kwon, K.; Jana, S.; Kim, S.; Avila-Crump, S.; Tae, G.; Mehl, R. A.; Kwon, I. Temporal Control of Efficient in Vivo Bioconjugation Using a Genetically Encoded Tetrazine-Mediated Inverse-Electron-Demand Diels-Alder Reaction. *Bioconjugate Chem.* **2020**, *31* (10), 2456−2464.

(18) Schlesinger, N.; Yasothan, U.; Kirkpatrick, P. Pegloticase. *Nat. Rev. Drug Discovery* **2011**, *10* (1), 17−18.

(19) Sundy, J. S.; Becker, M. A.; Baraf, H. S. B.; Barkhuizen, A.; Moreland, L. W.; Huang, W.; Waltrip, R. W.; Maroli, A. N.; Horowitz, Z. Reduction of Plasma Urate Levels Following Treatment with Multiple Doses of Pegloticase (Polyethylene Glycol-Conjugated Uricase) in Patients with Treatment-failure Gout: Results of a Phase II Randomized Study. *Arthritis & Rheumatology* **2008**, *58* (9), 2882−2891.

(20) Sundy, J. S.; Baraf, H. S. B.; Yood, R. A.; Edwards, N. L.; Gutierrez-Urena, S. R.; Treadwell, E. L.; Vázquez-Mellado, J.; White, W. B.; Lipsky, P. E.; Horowitz, Z.; Huang, W.; Maroli, A. N.; Waltrip, R. W.; Hamburger, S. A.; Becker, M. A. Efficacy and Tolerability of Pegloticase for the Treatment of Chronic Gout in Patients Refractory to Conventional Treatment. *Journal of the American Medical Association* **2011**, *306* (7), 711−720.

(21) Jumper, J.; Evans, R.; Pritzel, A.; Green, T.; Figurnov, M.; Ronneberger, O.; Tunyasuvunakool, K.; Bates, R.; Žídek, A.; Potapenko, A.; Bridgland, A.; Meyer, C.; Kohl, S. A. A.; Ballard, A. J.; Cowie, A.; Romera-Paredes, B.; Nikolov, S.; Jain, R.; Adler, J.; Back, T.; Petersen, S.; Reiman, D.; Clancy, E.; Zielinski, M.; Steinegger, M.; Pacholska, M.; Berghammer, T.; Bodenstein, S.; Silver, D.; Vinyals, O.; Senior, A. W.; Kavukcuoglu, K.; Kohli, P.; Hassabis, D. Highly Accurate Protein Structure Prediction with AlphaFold. *Nature* **2021**, *596* (7873), 583−589.

(22) Mirdita, M.; Schütze, K.; Moriwaki, Y.; Heo, L.; Ovchinnikov, S.; Steinegger, M. ColabFold: Making Protein Folding Accessible to All. *Nat. Methods* **2022**, *19*, 679−682.

(23) Chaudhury, S.; Lyskov, S.; Gray, J. J. PyRosetta: A Script-Based Interface for Implementing Molecular Modeling Algorithms Using Rosetta. *Bioinformatics* **2010**, *26* (5), 689−691.

(24) Liu, Z.; Zhou, H.; Wang, W.; Tan, W.; Fu, Y.-X.; Zhu, M. A Novel Method for Synthetic Vaccine Construction Based on Protein Assembly. *Sci. Rep.* **2014**, *4*, 7266.

(25) Li, L.; Fierer, J. O.; Rapoport, T. A.; Howarth, M. Structural Analysis and Optimization of the Covalent Association between SpyCatcher and a Peptide Tag. *J. Mol. Biol.* **2014**, *426* (2), 309−317.

(26) Gilmore, M. A.; Steward, L. E.; Chamberlin, A. R. Incorporation of Noncoded Amino Acids by In Vitro Protein Biosynthesis. In *Implementation and Redesign of Catalytic Function in Biopolymers*; Schmidtchen, F. P., Ed.; Topics in Current Chemistry; Springer: 1999; Vol. *202*, pp 77−99, DOI: 10.1007/3-540-48990-8_3.

(27) Andersen, J. T.; Dalhus, B.; Cameron, J.; Daba, M. B.; Plumridge, A.; Evans, L.; Brennan, S. O.; Gunnarsen, K. S.; Bjørås, M.; Sleep, D.; Sandlie, I. Structure-Based Mutagenesis Reveals the Albumin-Binding Site of the Neonatal Fc Receptor. *Nat. Commun.* **2012**, *3*, 610.

(28) Yang, B.; Kwon, I. Chemical Modification of Cysteine with 3-Arylpropriolonitrile Improves the In Vivo Stability of Albumin-

Conjugated Urate Oxidase Therapeutic Protein. *Biomedicines* **2021**, *9*, 1334.
(29) Caliceti, P. Pharmacokinetic and Biodistribution Properties of Poly(Ethylene Glycol)-Protein Conjugates. *Adv. Drug Delivery Rev.* **2003**, *55* (10), 1261−1277.
(30) Yang, B.; Kim, J. C.; Seong, J.; Tae, G.; Kwon, I. Comparative Studies of the Serum Half-Life Extension of a Protein: Via Site-Specific Conjugation to a Species-Matched or -Mismatched Albumin. *Biomaterials Science* **2018**, *6* (8), 2092−2100.
(31) Kim, S. Development of Multi Enzyme/Catalyst System for Industrial and Medical Application Using Polymeric Nanoplatform. Ph.D. Dissertiation, Gwangju Institute of Science and Technology, Gwangju, 2023.
(32) Pace, C. N.; Vajdos, F.; Fee, L.; Grimsley, G.; Gray, T. How to Measure and Predict the Molar Absorption Coefficient of a Protein. *Protein Sci.* **1995**, *4* (11), 2411−2423.
(33) Kim, S.; Kim, M.; Jung, S.; Kwon, K.; Park, J.; Kim, S.; Kwon, I.; Tae, G. Co-Delivery of Therapeutic Protein and Catalase-Mimic Nanoparticle Using a Biocompatible Nanocarrier for Enhanced Therapeutic Effect. *J. Controlled Release* **2019**, *309*, 181−189.
(34) Kim, S.; Kim, D. H.; Cho, J.; Kim, J.; Kwon, I. Charge Booster Tags for Controlled Release of Therapeutics from a Therapeutic Carrier. *Adv. Funct. Mater.* **2023**, *33* (11), 2209874.

https://doi.org/10.1021/acsomega.4c02303
ACS Omega 2024, 9, 22990−23000